Electron Beam Diagnostics Applied to High-Density Gasdynamic Laser Mixtures

S. L. Petrie*
The Ohio State University, Columbus, Ohio

A new, systematic study of the electron beam induced emission in N_2-CO_2-H_2O mixtures typical of those in gasdynamic lasers has been conducted. Vibrational temperatures of molecular nitrogen were successfully measured at density levels at least an order-of-magnitude above those normally used with an electron beam. The experimental studies were performed in an arc-heated free jet with densities up to those corresponding to a pressure of 20 torr at 300K. Comparisons of theoretical and experimental N_2 vibrational temperatures are presented which show that the data are not adversly influenced by the high density nor by the addition of CO_2 and H_2O so long as there is a relatively high flow velocity.

Nomenclature

$a_j, A, B, C,$
c_1, c_2, k_1, k_2 = intensity proportionality constants
A_{ij} = radiative transition probability for $i \rightarrow j$ transition
c = speed of light
h = Planck's constant
I_{jk} = intensity for $j \rightarrow k$ transition
I_{fs} = intensity of reference gas conditions
I_0 = intensity in the absence of collision quenching
k = Boltzmann's constant
L = electron beam path length
m_i = reduced mass of N_2 and species i particles
m = molecular weight
n_e = electron number density
n_g = gas number density
n_i = number density of species i
n_i' = quenching number density for species i
p = static pressure
p_e = equivalent pressure
Q_{oj} = cross section for excitation of N_2 to level j in the $N_2^+(B^2\Sigma)$ state due to electron beam excitation
Q_{ji} = cross section for collisions between N_2 molecules in level j and particles of species i
R = gas constant
T = translational temperature
v_e = electron velocity
V_e = electron beam accelerating potential
X = mole fraction of N_2
α = intensity constant
γ = frozen ratio of specific heats
ν_{jk} = wavenumber for the $j \rightarrow k$ transition
τ = vibrational relaxation time

Introduction

THE very efficient energy transfer between the asymmetrical stretch mode (ν_3) of CO_2 and N_2 is responsible, in part, for the population inversions which lead to lasing in the N_2-CO_2-H_2O (or He) gasdynamic laser (GDL). A widely used grouping of the energy states active in the GDL, due to Anderson,[1] is illustrated in Fig. 1. The vibrational relaxation of N_2 within a flowfield is relatively slow so that the resonant transfer between N_2 and the ν_3 mode of CO_2 leads to an elevated population of the (001) level of CO_2 compared to that of the (100) level. The population inversion is enhanced by the addition of H_2O or He which increases the rate of de-excitation of the (100) level.

To estimate GDL performance and optimize operating parameters, accurate values for the rates of the various kinetic processes must be available. Such information can be obtained only from direct measurements in expanding flowfields. The vibrational population distributions of CO_2 and H_2O can be investigated by measuring the intensities of the vibration-rotation bands emitted by these molecules. However, since N_2 is homonuclear, it has no pure vibration-rotation spectrum and some other means of investigating the vibrational population distribution must be used.

The electron beam provides a means for direct measurement of the vibrational temperature of N_2. In this technique, an electron beam generator produces a narrow column of high-energy (20 keV) electrons which is projected across the flowfield of interest. The interaction of the accelerated electrons with gas particles produces a column of radiation which is nearly coincident with the beam of electrons. Under appropriate conditions, the fluorescence can be analyzed spectroscopically to determine the concentration and temperature of the active species.

The predominant radiation due to excitation of N_2 is the first negative system of the ionized nitrogen molecule. The most intense band of this system is the (0,0) band at 3914 Å.

Much experimental work, summarized by Muntz,[2] has been done with the first negative system in nitrogen and air to verify the applicability of the diagnostic technique at sufficiently low density and high temperatures. It should be noted that the rotational line and vibrational band intensities in the first negative system are used in an excitation-emission analysis to determine the rotational and vibrational population distributions for the molecules in their ground electronic state. That is, the rotational and vibrational temperatures prior to excitation by the high-speed electrons are obtained. Details of the method can be found in Refs. 2-5. The electron beam technique has been applied previously to N_2-CO_2 mixtures,[6] but the measurements were made at gas densities much lower than those typical of operating GDL's. Since there is considerable interest in making direct measurements of the vibrational temperature of N_2 in actual GDL flowfields, techniques for applying the electron beam to high-density mixtures of N_2, CO_2 and H_2O were investigated.

Investigations of the accuracy with which the rotational and vibrational temperatures of molecular nitrogen can be

Presented as Paper 76-396 at the AIAA 9th Fluid and Plasma Dynamics Conference, San Diego, Calif., July 14-16, 1976; submitted Aug. 9, 1976; revision received Feb. 28, 1977.

Index categories: Nozzle and Channel Flow; Lasers; Research Facilities and Instrumentation.

*Professor, Department of Aeronautical and Astronautical Engineering.

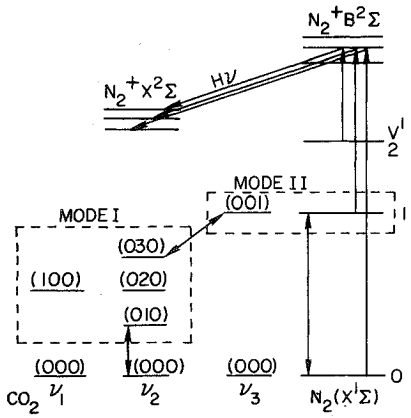

Fig. 1 Partial energy level diagram for the N_2-CO_2 system.

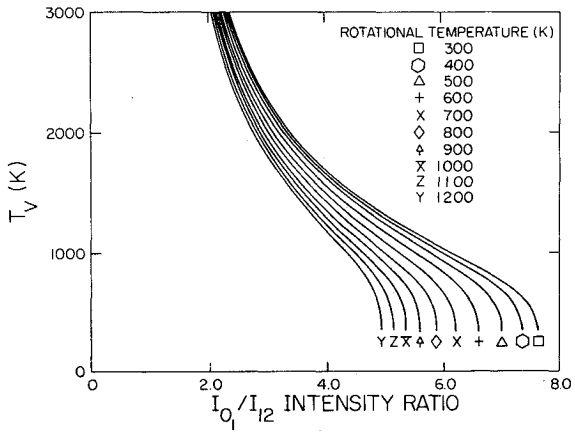

Fig. 2 Theroetical intensity ratios for the $N_2^+(0,1)$ and (1,2) vibrational bands.

measured in high density air flows have recently been conducted.[7] Calibration experiments were performed in a static test chamber and in an arc-heated free jet facility. These studies show that at pressures above approximately 3 torr (at 300K) in a static test chamber, the line and band intensities in the N_2^+ first negative system cannot be used for temperature and density measurements. Severe overlap of the first negative system by bands of the N_2 second positive system occurs and there is considerable excitation by low-energy particles (secondary electrons, N_2^+ ions, metastable particles, etc.) trapped within the static chamber. However, with high flow velocities typical of those in arc-heated wind tunnels, accurate measurements of the N_2 vibrational temperatures in air flows can be obtained at densities at least as high as those corresponding to a pressure of 20 torr at 300K.

The purpose of the present studies was to investigate the density range over which nitrogen vibrational temperatures can be measured with an electron beam in N_2-CO_2-H_2O gas mixtures. The CO_2 concentrations in air were varied from 0 to 25% (by volume) and the H_2O concentration was varied from 0 to 1%. Equivalent pressures ranged from 2.0 to 30 torr. (Equivalent pressure is defined as the pressure corresponding to the actual gas density at a translational temperature of 300K). All data discussed here were obtained in the arc-heated free jet facility; Ref. 7 can be consulted for results of the static chamber experiments and the special problems associated with this type of testing.

Theoretical Analyses

Electron Beam Theory

To interpret electron beam measurements in terms of vibrational temperatures, a detailed analysis of the excitation-emission process which leads to the observed radiation must be available. It is common to assume that the emission is excited by collisions between beam electrons and gas molecules in their ground electronic energy state. All other excitation processes (excitation by secondary electrons and low-energy ions, double excitation, cascading, etc.) and all selective quenching mechanisms are ignored. The resulting excitation and emission processes are shown schematically in Fig. 1.

With these assumptions, measurements of line and band intensities can be interpreted in terms of rotational and vibrational temperature. The rotational temperatures are usually obtained from the rotational lines in the N_2^+ (0,0) band, while vibrational temperatures are determined from scans of at least two bands [typically $N_2^+(0,1)$ and $N_2^+(1,2)$ at 4278 Å and 4235 Å respectively]. For vibrational temperature measurement, integration of the intensity distribution should be used to obtain accurate total band intensities.

At high rotational temperatures, the rotational lines corresponding to high rotational quantum numbers overlap the next band in the sequence. For example, rotational lines in the (0,1) band with rotational quantum numbers greater than 23 overlap the band head of the (1,2) band. This overlap of rotational lines must be included in the theoretical analysis to allow unambiguous interpretation of the measured band intensities in terms of vibrational temperature.

The band intensity ratios for the (0,1) and (1,2) bands, including the effect of overlap due to high rotational temperatures, are given in Fig. 2. It is to be noted that significant errors in indicated vibrational temperature occur when the overlap accompanying high rotational temperature is ignored. All of the vibrational temperature data reported here were obtained from Fig. 2 employing the measured rotational temperatures and the integrated (0,1) and (1,2) vibrational band intensities.

In most applications of an electron beam, the gas densities are low enough that direct excitation by primary beam electrons is the only excitation mechanism and collision quenching of the electronic energy level excited by the beam can be ignored. However, in flows with densities typical of those in GDL's, the beam-induced radiation is highly quenched by collisional mechanisms.

The influence of collisions on the intensity resulting from electron beam excitation can be derived by requiring a steady-state population of the upper level of the observed transition assuming that only direct excitation, radiative transitions, and collision quenching occur. For simplicity, the rotational and vibrational structures of the radiation are ignored so that we deal only with the electronic transitions. A slight modification of the intensity formula given by Muntz[2] is

$$I_{jk} = \frac{hc\nu_{jk}(A_{jk}/A_T)\, n_e v_e Q_{0j}(v_e)\, n_g X}{1+\Sigma_i (2/A_T)\, n_i Q_{ji}(T)\,\{2kT\bar{m}_i/\pi\}^{1/2}} \qquad (1)$$

The summation over the index i must include all species which can quench the observed radiation. For constant electron beam current density and beam energy, Eq. (1) can be simplified to

$$I_{jk} = \frac{a_j n_g X}{1+\Sigma_i n_i/n_i'(T)} \qquad (2)$$

where

$$1/n_i'(T) = (2/A_T)\, Q_{ji}(T)\,\{2kT\bar{m}_i/\pi\}^{1/2} \qquad (3)$$

$n_i'(T)$ is defined as the quenching density analogous to the quenching pressure defined by Grün.[8] In a single-species gas, when the density is equal to $n_i'(T)$, the intensity is reduced to one-half the value obtained in the absence of collision quenching.

In GDL flowfields, the density is expected to be high enough that the terms in the summation of Eq. (2) dominate the denominator. In the limit of very high gas density, Eq. (2)

becomes

$$I_{jk} = \frac{a_j n_g X}{\Sigma_i n_i / n_i'(T)} \tag{4}$$

As discussed by Grün,[8] in the high-density limit for a single species gas or if one term dominates the summation of Eq. (4), the intensity becomes independent of the absolute number density of the excited species and becomes a function of temperature (through the unique dependence of n_i' on temperature) and the relative concentrations of the excited and quenching species, i.e.,

$$I_{jk} = a_j n_i'(T) X / X_i \tag{5}$$

In studies similar to those discussed here, Smith and Driscoll[9] employed a form of Eq. (1) written for high-density helium ($X=1$) as

$$I_{jk} = \frac{k_1 n_g}{1 + k_2 n_g Q(T) \{(8/\pi) RT\}^{1/2}} \tag{6}$$

In this notation, the quenching density would be given by $1/n'(T) = k_2 Q(T) \{(8/\pi) RT\}^{1/2}$. Smith and Driscoll simplified Eq. (6) to

$$I/I_{fs} = [c_1 n_g / (1 + c_2 n T^{\alpha})] \tag{7}$$

and experimentally evaluated c_1, c_2, and α for several helium lines at translational temperatures from 3.5 to 300K. They demonstrated that simultaneous time-resolved measurements of both the helium density and translational temperature can be obtained in high-density helium flows when quenching is an important mechanism.

Alternate correlations for Eq. (6) have been developed. For helium[10] and nitrogen,[11] an equation in the form

$$I_{jk} = (A n_g + B n_g^2) / (1 + C n_g T^{\alpha}) \tag{8}$$

has been used to fit experimental data. The second term in the numerator of Eq. (8) accounts for excitation by secondary electrons and collisional exchange with excited particles in other energy states. Detailed expressions for the second term are given by Muntz.[2]

In the present work, we are concerned with making vibrational temperature measurements, rather than density determinations. Since temperatures are obtained from measurements of the *relative* intensities of the vibrational bands, Eq. (2) is written in the form

$$\frac{I_{jk}}{I_{\ell m}} = \frac{I_{ojk}}{I_{o\ell m}} \times \frac{1 + \Sigma_i n_i / n'_{\ell i}(T)}{1 + \Sigma_i n_i / n'_{ji}(T)} \tag{9}$$

where I_0 is the intensity which would be observed if there were no quenching. Separated quenching densities are defined for the vibrational energy levels in the excited electronic energy state; $n'_{\ell i}(T)$ denotes the quenching density of the ℓth vibrational energy level due to collisions with species i. While the extent of the quenching will vary with both the absolute number density and the translational temperature, the central question in application of the technique to vibrational temperature measurement is whether the ratio of quenching terms in Eq. (9) will vary with density. That is, vibrational temperatures can be measured in the presence of severe quenching if the $n_{\ell i}'(T)$ values in Eq. (9) are constant for all vibrational levels in the $N_2^+(B^2\Sigma)$ state. The experimental studies discussed here were directed at examining the accuracy with which vibrational temperatures can be measured in N_2-CO_2-H_2O mixtures when the intensities resulting from electron beam excitation of N_2 must be represented in the form of Eq. (9).

Vibrational Relaxation Model

To evaluate the accuracy of vibrational temperature measurements, a reliable model of the vibrational relaxation process which occurs in the flowfield must be available. The model of Anderson[1] was modified to provide theoretical estimates of the N_2 vibrational temperatures at the measuring stations. The various kinetic rates given in Ref. 12 were employed, except for the N_2-N_2 rate. The N_2-air rate of Sebacher[13] given by

$$\tau p(\text{sec-atm}) = 1.2 \times 10^{-10} \exp(130 T^{-1/3}) \tag{10}$$

was used in place of the N_2-N_2 rate and the vibrational temperature of O_2 was set equal to that of N_2. No effects of O_2 on collisional deactivation of the other energy levels were included.

While ignoring the effects of O_2 on all levels except the vibrational levels of N_2 in the $(X^1\Sigma)$ state will lead to some error in predicting the CO_2 vibrational relaxation, the effects on the predicted translational temperature are expected to be minimal. The main consideration here is to predict the N_2 vibrational temperature variation through the flowfield and the rate of Eq. (10) has been shown to apply with good accuracy, particularly for reservoir temperature above 2000K.[13]

As described in the next section, the experimental configuration consisted of a conical nozzle exhausting to an open-jet test cabin. For the conditions of these studies, the nozzle flow was highly underexpanded so that a strong expansion wave system emanated from the nozzle exit. The N_2 vibrational relaxation was assumed to proceed only up to the point where the leading expansion wave from the nozzle exit crossed the nozzle centerline. All vibrational temperatures downstream of this freezing point were assumed to be equal to their values at the freezing point. Theoretical variations of the temperatures through the nozzle and the locations of the nozzle exit and freezing point are given in Fig. 3 for the highest reservoir temperature used. The theoretical temperatures resulting from an earlier[14] N_2-N_2 rate are included in Fig. 3 to indicate the difference between N_2-N_2 and N_2-air vibrational relaxation. At lower reservoir temperatures, the differences between the two sets of theoretical results diminish.

The gas conditions at the measuring stations were determined by measuring the local pitot pressure. The theoretical model of Ref. 1 was modified to include a pitot pressure calculation. This was accomplished by assuming that the flow through the pitot probe shock wave was vibrationally frozen. A frozen speed of sound was calculated from

$$a_f = \sqrt{\gamma RT/m} \tag{11}$$

The Mach number obtained from a_f and the local velocity was then used in an isentropic formula to compute the ratio of pitot and freestream static pressures. The values for the flow

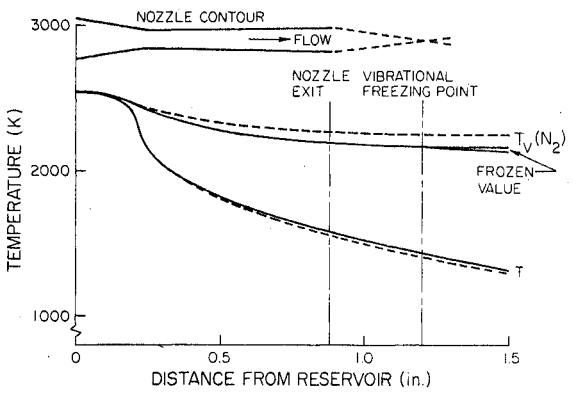

Fig. 3 Theoretical temperature distributions at a reservoir pressure of 1 atm; τp from Eq. (10);---τp from Ref. 14.

properties at the measuring stations were obtained from this theoretical model by matching the theoretical and experimental pitot pressure ratios.

Experimental Apparatus and Procedures

Arc-Heated Free Jet

An arc-heated free jet facility was employed to provide air flows at known thermodynamic conditions. In certain cases, unheated CO_2 was admixed with arc heated air upstream of the nozzle. Molecular hydrogen was also added to provide H_2O with the water-gas reaction.

A conical nozzle was employed with an expansion half angle of 3.5°, delivering a flow with a nominal Mach number of 2.0 and a static pressure of 60 torr. The vacuum pumping station maintained a pressure in the free jet test cabin of approximately 0.5 torr; hence, a "barrel-shock" system was generated by the highly underexpanded nozzle flowfield. The electron beam was projected across the flowfield at various distances downstream of the nozzle exit to provide test regions with static pressures varying from 1.5 to 60 torr and flow Mach numbers from 2.0 to 4.25.

Electron Beam System

The electron beam was generated by a commercially available 19AYP4 television electron gun. Beam currents of approximately 0.5 mA at voltages near 15 kV were employed. The entire electron beam generator system was electrically isolated from the wind tunnel so that no special beam collecting device was required.

Rotational and vibrational spectra were obtained with a Jarrell-Ash 0.5 Meter Ebert scanning spectrometer. The grating was ruled with 30,000 lines/in. yielding a dispersion of 16 Å per millimeter and a maximum resolution of 0.2 Å. An uncooled EMI 6256 photomultiplier was used with the spectrometer.

The image of the electron beam was focused on the entrance slit of the spectrometer by a 13 in. focal length, 2 1/2 in. diameter quartz lens. The electron beam was oriented perpendicular to the entrance slit. Photocurrents were measured and amplified by a Keithly Model 417 picoammeter. The output of the amplifier was entered into the signal conditioning system of the Digital Computer and Data Acquisition System operated by The Aeronautical and Astronautical Research Laboratory of the Ohio State University.

The electron beam current was continuously monitored by a second photomultiplier-spectrometer system. Radiation from the electron beam was focused on the entrance slit of a 0.25 m Jarrell-Ash spectrometer set to view the head of (0,0) band of the N_2^+ first negative system at 3914 Å.

During all spectral scans, the output from the 0.5 m spectrometer was divided by that from the 0.25 m spectrometer to account for variations in beam current during the wavelength scan. All data reported here were obtained in this manner. A schematic of the optical system is given in Fig. 4.

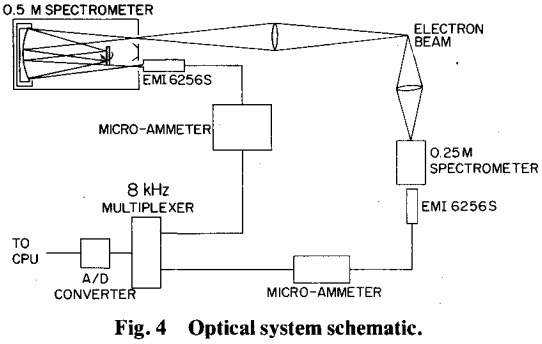

Fig. 4 Optical system schematic.

Because of the relatively high flow densities and low beam voltage employed for these studies, beam spreading was a potential problem. In this case, the main effect of beam spreading is a loss of spatial resolution, which could be important because of the large gradients in flow properties present within the free jet. A series of experiments was performed to determine the variation of beam diameter with beam voltage, gas density, and path length. The data were obtained in a static test chamber for voltages from 10 to 40 kV, pressures from 0.2 to 30 torr, and path lengths up to 6 in. The results of these experiments are reported in detail in Ref. 7. The data are well-correlated by expressing the change in radiation half width of the beam as

$$\Delta W/L = 0.44\,[p_e(\text{torr})L(\text{cm}/V_e^2(\text{kV})]^{1/2} \qquad (12)$$

ΔW gives the difference between the half width and the minimum beam half-width, which usually occurs at the exit orifice of the beam generator. The results given by Eq. 12 agree in form with those given by Camac[15] and Wallace[16] except that here the change in beam half-width is correlated rather than the half-width itself.

For the measurements reported here, density variations were obtained by examining various locations within the highly underexpanded free-jet. Because of the low density of the gas surrounding the free-jet, very little beam spreading occurred up to the point where the beam entered the free-jet. At the highest density condition (equivalent pressure of 30 torr), the beam path length within the gas was approximately 5 mm; hence, the beam half-width increased by 0.5 mm, giving a total beam diameter at the measuring station of approximately 3 mm. At the lowest density condition of 1 torr, the path length through the free jet was about 25 mm, leading to a beam diameter of approximately 5 mm. Hence, the beam spreading did not result in significant loss of spatial resolution in the flow direction.

Results and Discussion

Test Conditions

Wind tunnel data were obtained at axial locations downstream of the nozzle exit approximately equal to 0.10, 1.5, and 2.0 in. At each of these positions, the reservoir temperature was varied from approximately 1500K to 2200K at a nominal reservoir pressure of 1.0 atm. To ensure that pitot pressure and electron beam data were taken at the same position within the flowfield, the electron beam was always positioned such that it intersected the tip of the probe while the probe was positioned on the tunnel centerline. The beam position was adjusted with a deflection coil mounted between the exit orifice of the drift tube and test region. Once the

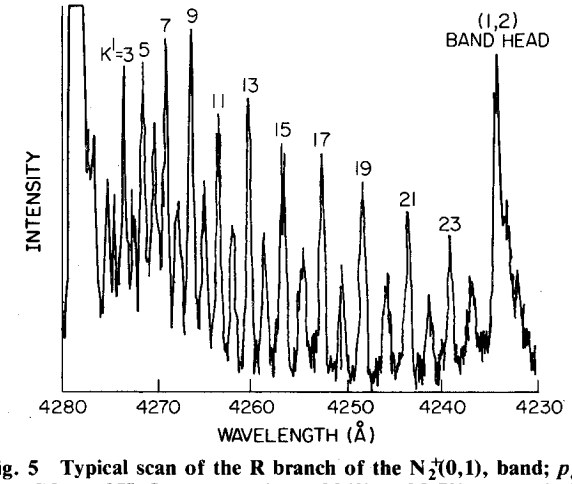

Fig. 5 Typical scan of the R branch of the $N_2^+(0,1)$, band; $p_e = 20$ torr; CO_2 and H_2O concentrations of 24% and 0.7%, respectively.

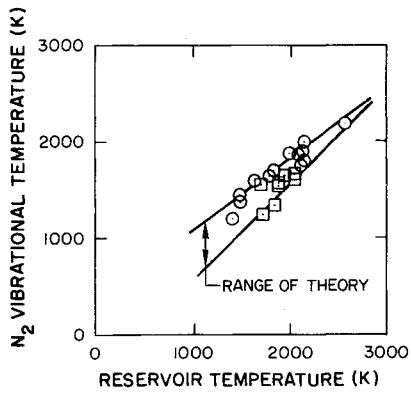

Fig. 6 Summary of measured N_2 vibrational temperatures.

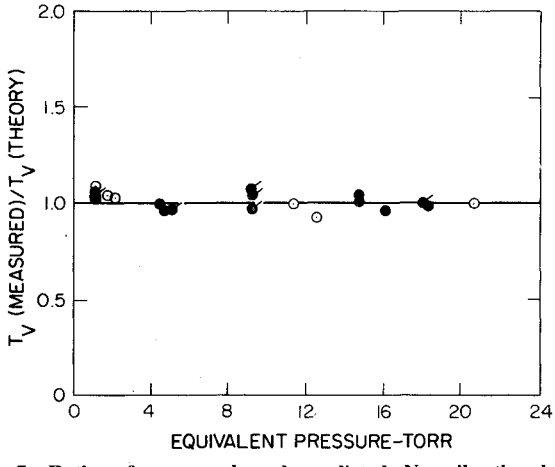

Fig. 7 Ratio of measured and predicted N_2 vibrational temperatures; o air; ● air + CO_2; ◤ air + CO_2 + H_2O.

proper alignment was achieved, the pitot probe was withdrawn and spectral data were collected.

Spectral Features

The rotational structures of the (0,0), (0,1), and (1,2) bands of the first negative system were examined in detail to determine if excitation by secondary electrons or preferential collision quenching disturbs the band structure in a high-density air flow containing CO_2 and H_2O. A typical scan of the R-branch of the (0,1) band obtained at an equivalent pressure of approximately 20 torr with CO_2 and H_2O concentrations of approximately 24% and 0.7%, respectively, is shown in Fig. 5.

The band profile agrees well with the results of theoretical predictions ignoring preferential collision quenching and excitation by secondary electrons. It also agrees well with scans obtained at low densities where quenching can be ignored.

The studies reported in Ref. 7 for N_2 in air show that the (0,1) band is overlapped severely by the (1,5) band of the N_2 second positive system under static (no flow) conditions. It is apparent that in the static chamber at high densities the second positive system is excited by long-lived metastable species which remain within the field of observation. However, in a high-speed flowfield, these species are swept from the field of view and do not appear to contribute to the excitation in any measurable way for the gas conditions of these studies. Similarly, no measurable influence of preferential collision quenching of the vibrational energy levels in the $N_2^+(B^2\Sigma)$ state could be observed. The addition of CO_2 and H_2O to the flowfield does not appear to alter these conditions.

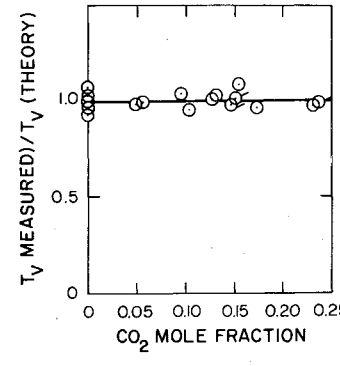

Fig. 8 Ratio of measured and predicted N_2 vibrational temperatures for various CO_2 mole fractions; o air + CO_2; σ air + CO_2 + H_2O.

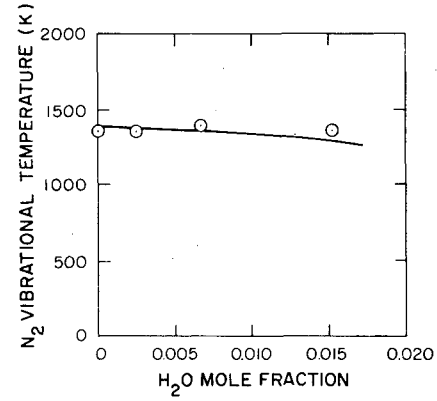

Fig. 9 N_2 vibrational temperature in N_2-H_2O mixtures; o experimental data; —theoretical temperatures.

Thermodynamic Data Comparisons

The measured N_2 vibrational temperatures are compared with the theoretical estimates in Fig. 6. The range in predicted temperatures is due to the variations in reservoir pressures accompanying varying mixture ratios and the influences of CO_2 and H_2O addition on the theoretical N_2 vibrational relaxation. Good overall agreement of the theoretical and experimental data is evident in Fig. 6.

To determine the possible effects of selective quenching on the data, the ratios of the measured and predicted N_2 vibrational temperatures are shown in Fig. 7 plotted against equivalent pressure. No specific trend in the ratio of the measured and predicted temperatures with gas density is evident. At equivalent pressures greater than approximately 1 torr, the radiation in the N_2^+ first negative system is highly quenched by collisional mechanisms. However, the data of Fig. 7 demonstrate that the rotational and vibrational energy levels in the $N_2^+(B^2\Sigma)$ electronic energy state are not preferentially quenched for equivalent pressures at least up to 20 torr.

The scatter in the data of Fig. 7 amounts to approximately ±6% and is due to accumulation of errors in determining the reservoir temperature from the measured mass flow rates and reservoir pressure, uncertainties in determining the rotational temperature (for use with Fig. 2 to determine vibrational temperature), and inaccuracies in obtaining integrated band intensities.

Ratios of the measured and predicted nitrogen vibrational temperatures in various air-CO_2-H_2O mixtures are given in Fig. 8 as functions of the mole fraction of CO_2 in the mixture. Good agreement between the predicted and measured temperatures is evident, indicating that the presence of CO_2 in the gas mixture causes no additional perturbations in the electron beam induced radiation in the N_2^+ first negative bands used in this study. In addition, the presence of CO_2 does not appear to lead to measurable excitation of the N_2^+ first negative system by secondary electrons.

The effects of the addition of water vapor on the measured temperatures are shown in Fig. 9. These data were obtained with no CO_2 in the flow and reflect the influence of the N_2-H_2O vibrational relaxation rate on the N_2 vibrational temperature distribution. The theoretical predictions show that the addition of small quantities of H_2O has only a minor influence on the nitrogen vibrational temperature. The difference between the measured and predicted temperatures are within the accuracy of the measurements; however, the trend to the data suggests that a systematic error in either the measured temperatures, the predicted temperatures, or both may exist.

Conclusions

A new, systematic study of the electron beam induced emission in N_2-CO_2-H_2O mixtures has been conducted at density levels well above those normally used in application of the technique. In the density range investigated, the comparisons of the theoretical and experimental N_2 vibrational temperatures show that the data are not influenced by selective collision quenching nor by excitation by secondary particles in any measurable amount when there is sufficient flow velocity to sweep long lived metastable particles out of the region of observation. Hence, in the temperature and density ranges of these studies, it is concluded that vibrational temperatures can be measured in typical GDL gas mixtures with no loss in accuracy for equivalent pressures at least up to 20 torr.

Acknowledgment

This research was supported by the Air Force Weapons Laboratory and the Air Force Office of Scientific Research under Grant No. 73-2537.

References

[1]Glowacki, W. J. and Anderson, J. D., "A Computer Program for CO_2-N_2-H_2O Gas Dynamic Laser Gain and Maximum Available Powers," Naval Ordnance Lab., White Oak, Silver Spring, Md., NOLTR-71-210, 1971.

[2]Muntz, E. P., "The Electron Beam Fluorescent Technique," AGARDograph 132, 1968.

[3]Petrie, S. L., "Density Measurements with Electron Beams," *AIAA Journal*, Vol. 4, Sept. 1966, pp. 1679-1680.

[4]Petrie, S. L., Boiarski, A. A., and Lee, H. F., "Electron Beam Flow Field Analyses in the AFFDL 2-Ft. Electrogasdynamics Facility," Air Force Flight Dynamics Lab., Wright Patterson AFB, Ohio, AFFDL-TR-71-161, 1971.

[5]Petrie, S. L., Boiarski, A. A., and Lazdinis, S. S., "Electron Beam Studies of the Properties of Molecular and Atomic Oxygen," Air Force Flight Dynamics Lab., Wright Patterson AFB, Ohio, AFFDL-TR-71-30, 1971.

[6]Sebacher, D. I., Guy, R. W., and Lee, L. P., "Vibrational Energy Transfer in Expanding Mixtures of N_2 and CO_2 as Measured by an Electron Beam," NASA TN D-64451, 1971.

[7]Petrie, S. L., "Application of an Electron Beam to Temperature Measurements at High Densities," Air Force Flight Dynamics Lab., Wright Patterson, AFB, Ohio, AFFDL-TR (to be published).

[8]Grün, A. E., "On the Fluorescence of Air, Excited by Fast Electrons: Light Yield as a Function of Pressure," *Canadian Journal of Physics*, Vol. 36, 1958, p. 858.

[9]Smith, J. A. and Driscoll, J. F., "The Electron-Beam Flouresence Technique for Measurements in Hypersonic Turbulent Flows," *Journal of Fluid Mechanics*, Vol. 72, 1975, p. 695.

[10]Hunter, W. W. and Leenhardt, T. E., "Temperature Dependence of the 3^1 P Excitation Transfer Cross Section of Helium," *Journal of Chemical Physics*, Vol. 58, 1973.

[11]Harvey, W. D. and Hunter, W. W., "Experimental Study of Free Turbulent Shear Flow at Mach 19 with Electron Beam and Conventional Probes," NASA TN D-7981, 1975.

[12]Anderson, J. D., "The Effects of Kinetic Rate Uncertainties on Gasdynamic Laser Performance," AIAA Paper 74-176, Washington, D.C., 1974; also *AIAA Journal*, Vol. 12, Dec. 1974, pp. 1699-1703.

[13]Sebacher, D. I. and Guy, R. W., "Vibrational Relaxation in Expanding N_2 and Air," NASA TM X-71988, 1974.

[14]Sebacher, D. I., "A Correlation of N_2 Vibrational, Translational Relaxation Times," *AIAA Journal*, Vol. 5, April 1967, pp. 819-820.

[15]Camac, M., "Boundary Layer Measurements with an Electron Beam," AVCO Research Rept. 275, 1967.

[16]Wallace, J. E., "Hypersonic Turbulent Boundary Layer Measurement Using an Electron Beam," Cornell University, Ithaca, N.Y., Cornell Aero Lab Rep. AN-2112-4-1, 1968.